

## Single crystal EPR studies on low dimensional ferromagnet cyclohexylammonium copper bromide

Sarmila Datta, A K Pal\* and Dipali Banerjee<sup>1</sup>

Department of Solid State Physics, Indian Association for the Cultivation of Science,  
Jadavpur, Calcutta-700 032, India

<sup>1</sup>Department of Physics, B. E. College (D.U.), Howrah-711 103, West Bengal, India

E-mail : sspakp@mahendra.iaacs.res.in

**Abstract** The title compound (CHAB, in brief) is one of the best realisations of 1D,  $S = 1/2$  Heisenberg like ferromagnet as evidenced by the specific heat studies and the existence of a 3D ordering temperature at 1.50 K. EPR linewidths in several crystallographic planes are measured at X-band, at room temperature and LNT temperature and analysed on the basis of the anisotropic exchange theories of McGregor and Soos and Ritter *et al* to shed light on the spin dynamics in CHAB. The principal findings are:

- (i) Anisotropic antisymmetric exchange ( $1.47 \text{ cm}^{-1}$ ) is of the same order of magnitude as that of the anisotropic symmetric exchange ( $1.21 \text{ cm}^{-1}$ ). This indicates that the well known Moriya relations regarding anisotropic exchange interaction requires revision.
- (ii) The z-direction of the anisotropic antisymmetric exchange is along the b-axis of the orthorhombic crystal *ie* at right angles to the chain axis (c-axis).
- (iii) Pronounced orthorhombicity in the anisotropic symmetric exchange tensor is indicated.

Principal ionic g-factors are evaluated from crystalline g-factors and the nature of the ligand field in this ionic compound has been discussed.

**Keywords** EPR, ferromagnet, low-dimensional magnetism

**PACS Nos.** : 76.30.-v, 75.20.-g, S13, S1.3

### 1. Introduction

In recent times, extensive investigations, both theoretical and experimental, on the magnetism of low-dimensional (low-D) transition metal compounds [1-3], have been carried out. EPR lineshape and linewidth studies have been of immense help in understanding the spin dynamics and magnetic interactions in low-D compounds, specially,  $\text{Mn}^{2+}$  systems in terms of spin-diffusion theory [4-7]. In  $\text{Cu}^{2+}$  systems so far studied, however, always some deviations from predictions of the ideal spin-diffusion theory have been observed. Soos and coworkers [8] have shown that besides magnetic dipolar interactions, anisotropic symmetric exchange (a.s.e) and anisotropic antisymmetric exchange (a.a.e.) interactions are required to be considered in explaining the linewidth anisotropy in some 1D and 2D copper systems. Structural studies [9, 10] indicate that copper cyclohexylammonium bromide (in brief, CHAB) is composed of linear chains of copper ions lying on the  $2_1$  axis parallel to the c-axis of the orthorhombic crystal having space group  $P2_12_12_1$  (Figure 1). The adjacent  $\text{Cu}^{2+}$  ions in a chain are

not magnetically equivalent while adjacent ions in chains lying side by side are equivalent. Each Cu atom is coordinated to five

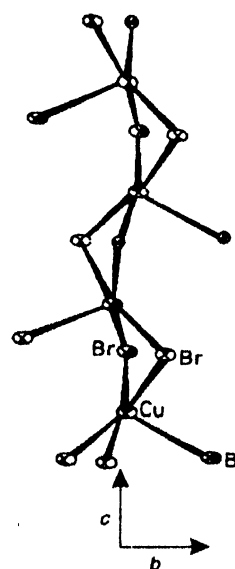


Figure 1. Infinite linear chain along c-axis of the orthorhombic crystal of CHAB.

\* Corresponding Author

Br<sup>-</sup> ligands in a nearly perfect square pyramidal geometry having C<sub>4v</sub> symmetry. The equatorial Cu-Br bonds participate in forming two symmetrical bridges between adjacent copper ions along the chain and serve as the superexchange pathways. The nearest intra-chain Cu-Cu distance is 3.234 Å. The Cu-atoms along the a-direction are separated by cyclohexylammonium (CHA) cations and the interchain distance is 10.7 Å. In the b-c plane along the b-direction, NH<sub>3</sub><sup>+</sup> radicals of the cyclohexyl ammonium groups keep the chains far apart (8.7 Å). So, structurally, the title compound can be considered as good one-dimensional compound. From single crystal ac susceptibility and magnetisation measurements in the temperature range 0.5–290K [11], an isotropic exchange parameter (J) of 37.8 cm<sup>-1</sup> along the chain has been derived. A similar value of J is also obtained from specific heat measurements in the temperature range 0.4–55K [12]. Slight anisotropy (~5%) in the isotropic exchange which is XY type has been confirmed in magnitude and nature by FMR experiments [13].

Present single crystal EPR studies of CHAB are carried out with a view to examine how far the observed linewidth anisotropy and lineshape in different planes of these crystals tally with the predictions of 1D spin diffusion theory. Further, analysis of these data has been attempted on the basis of the theories of McGregor and Soos [8] and Ritter *et al* [14]. Such analysis is expected to provide estimation of some finer aspects of exchange phenomena such as a.s.e. and a.a.e. interactions besides isotropic exchange. From principal ionic g-factors, the nature of the ligand field in this ionic compound is also assessed.

## 2. Experimental

Single crystals of CHAB are grown by slow evaporation at room temperature from an equimolecular solution of cyclohexylammonium bromide and anhydrous copper bromide in l-propanol. Dark needle-like crystals with needle axis parallel to the c-axis are obtained. With the help of a Varian E-line (E-109) Century Series X-band EPR Spectrometer, EPR spectra in three crystallographic planes (010), (100) and (001) are recorded at room and at liquid nitrogen (LN<sub>2</sub>) temperatures.

## 3. Results and discussion

### 3.1 Principal crystalline and ionic g-tensors :

From measurements in (010) and (100) planes, the principal crystalline g-factors,  $g_a$ ,  $g_b$ , and  $g_c$  are obtained where  $g_a$ ,  $g_b$ ,  $g_c$  are principal crystalline g-factors along a, b and c-axes respectively. The principal crystalline g-factors remain identical at room and LN<sub>2</sub> temperatures. EPR signals due to two magnetically inequivalent Cu<sup>2+</sup> complexes in the unit cell are not resolved, and so the simplifying assumption of tetragonal symmetry of the ligand field around each copper (II) ion is required to derive the principal ionic g-factors ( $g_{||}$  and  $g_{\perp}$ ) from

the principal crystalline g-factors with the help of the following relations :

$$g_{||}^2 - g_{\perp}^2 = (ga^2 - gb^2)/(\alpha_1^2 - \beta_1^2) \\ = (gb^2 - gc^2)/(\beta_1^2 - \gamma_1^2) = (gc^2 - ga^2)/(\gamma_1^2 - \alpha_1^2) \quad (1)$$

$$g_{||}^2 + 2g_{\perp}^2 = ga^2 + gb^2 + gc^2, \quad (2)$$

where  $\alpha_1$ ,  $\beta_1$ ,  $\gamma_1$  are the direction cosines of  $g_{||}$ -direction with respect to a, b, c axes of the crystal. Values of  $g_{||}$ ,  $g_{\perp}$  so derived are shown in Table 1. For fruitful assessment of the ligand field in this crystal, optical data are also required. Unfortunately, crystals of CHAB are quite opaque and so in absence of any dilutant diamagnetic isomorph, optical measurements of the ligand field bands could not be carried out. For the sake of comparison, g-factors of a similarly constituted halogen co-ordinated crystal, namely, square planar Cu<sup>2+</sup>: K<sub>2</sub>PdBr<sub>4</sub> [15] are included in the Table 1. Optical data for this crystal is also available [15]. Rigorous ligand field analysis of Aramburu and

Table 1. Principal ionic g-factors ( $g_{||}$ ,  $g_{\perp}$ )

Compound	Ligand Conformation	$g_{  }$	$g_{\perp}$
CHAB	Square – pyramidal	2.140	2.050
Cu <sup>2+</sup> :K <sub>2</sub> PdBr <sub>4</sub>	Square – planar	2.143	2.043

Moreno [15] which also takes care of ligand spin-orbit (s-o) coupling as well as charge transfer interaction has revealed that in case of bromine co-ordinated Cu<sup>2+</sup>: K<sub>2</sub>PdBr<sub>4</sub> [ $g_{||}$ ,  $g_{\perp}$ ] tensor is dominated by the charge transfer contribution while the ligand field contribution is quite small and negative. From Table 1, it is seen that both Cu<sup>2+</sup>: K<sub>2</sub>PdBr<sub>4</sub> and CHAB have very similar g-values (2.14). Thus, the ligand fields may be different but the differences should not affect the g-factor if Aramburu and Moreno's [15] theory is also applicable in case of CHAB and from the same argument it follows that the primary factor responsible for the observed  $g_{||}$ -values is charge transfer.

### 3.2 Lineshape and linewidth anisotropy :

Lineshape analysis shows that in all directions including the chain (c-axis) and the magic angle (54.7° to c-axis) directions the lineshape is Lorentzian. Derivative linewidths measured in (010), (100) and (001) planes are plotted *versus* orientation in Figures 2(a, b, c). It is noted that the linewidth is minimum (9.8 mT) along the chain axis and maximum (15mT) at an angle 90° to the chain axis. The above observations on lineshape and linewidth are clearly at variance with the predictions for a truly 1D spin-diffusion system which states that (i) the lineshape is non-Lorentzian along the chain axis, while it is Lorentzian at the magic angle and (ii) linewidth is maximum along the chain axis and minimum at the magic angle and shows a second maximum at an orientation 90° to the chain axis. Since the chains are structurally far apart (10.7 Å and 8.7 Å along a axis and b-axis respectively), the interchain exchange (denoted by J<sub>i</sub>) is expected

to be small and has little effect on the lineshape. This is confirmed from susceptibility and specific heat measurements of  $J_1$  at low

temperatures [10, 12].  $J_1$  is about three orders of magnitude smaller than intrachain exchange parameter  $J$ . Cu(II) ion has a large spin-orbit coupling ( $\lambda = -830 \text{ cm}^{-1}$ ) and it follows that both a.s.e. and a.a.e interactions (since copper sites in a chain lack inversion symmetry, Figure 1) may be present and are expected to play important roles in regulating the linewidth behavior of the present Cu(II) 1D FM system. It is also possible that a.s.e and a.a.e interactions also cause deviation of the lineshape from its ideal spin diffusion behaviour (interchain exchange is negligibly small). Soos and others [8, 14] took cognizance of anisotropic exchange interactions in formulating a comprehensive linewidth theory for Cu(II) low D systems. Their theories have been adopted in the present analysis.

McGregor and Soos [8] calculated the width of the EPR line by using general linewidth theory [16, 17] for a Cu(II) 1D system by including the Blume-Hubbard [18] result for spin-dynamics and preferentially weighting a.s.e and dipolar terms in one dimension. Ritter *et al* [14] extended the theory to situations where the symmetry of a.s.e is orthorhombic and in addition a.a.e. interaction is present. In case of CHAB, except the two neighbouring sites in a chain, all other sites are situated at large distances and the magnetic dipolar contributions due to them have been ignored in the second moment calculation. Since the nearest neighbours in a chain are quite close, the hyperfine interaction term in comparison to dipolar terms can be neglected. The non-secular contributions of the dipolar and a.s.e. terms to the second moment in the coordinates of Figure 3 is given by [14]

$$M_2' = \frac{3S(S+1)}{h^2} \left[ \frac{1}{3}(D_e/3)^2 \{ (3-2\Delta)\cos^2 \gamma' + (3+2\Delta) \} + D_d^2 (\cos^2 \theta + 1) - (D_e D_d / 3) \left\{ (3+\Delta)\cos^2 \gamma' - (1+\Delta) \right\} (3\cos^2 \theta - 1) + (1/3) [-2\Delta + (3+\Delta)\sin^2 \gamma'] \sin^2 \theta \cos [2(\alpha + \varphi)] \right] \quad (3)$$

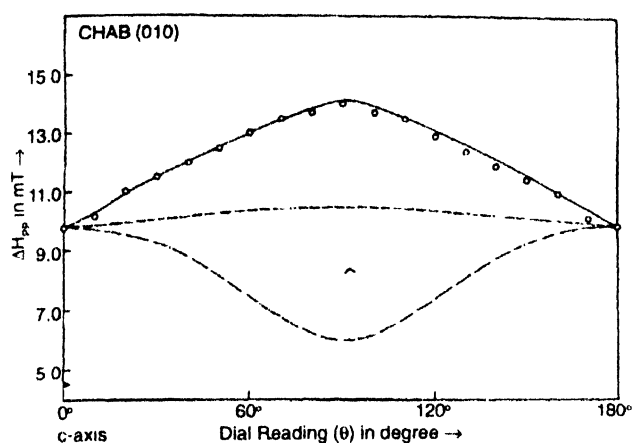
where

$$D_d = (\bar{g}\beta)^2 / r^3 \quad (4)$$

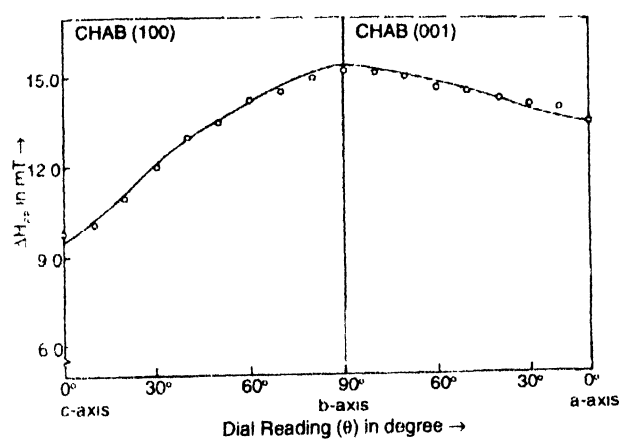
$$\text{and } g^2 = (g_a^2 + g_b^2 + g_c^2) / 3, \quad (5)$$

where  $r$  is the nearest -neighbour intrachain separation along the chain axis ( $z$ ).  $D_e$  and  $\Delta$  are respectively the axial and orthorhombic components of the a.s.e tensor. The angle  $\alpha$  represents the rotation of  $D_e^{mol}$  (a.s.e. tensor in the molecular frame) about  $Z$  (the  $z$ -direction of the principal  $g$ -tensor) which results from the transformation to laboratory co-ordinates,

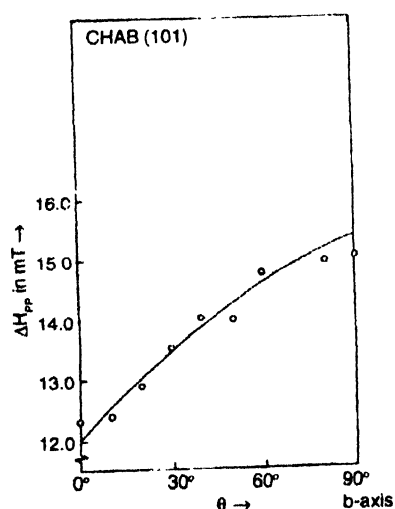
$$D_e^{mol} = (De)/3 \begin{vmatrix} q & 0 & 0 \\ 0 & p & 0 \\ 0 & 0 & 2 \end{vmatrix} \quad (6)$$



2(a)



2(b)



2(c)

Figure 2. Derivative linewidths ( $\Delta H_{pp}$ ) vs orientation ( $\theta$ ) in the (a) (010), (b) (100) and (001), (c) (101) planes of CHAB.

(00) Experimental points

(-o-o-) : a.s.e. having axial symm.+non-zero  $\rho$  and  $\alpha$

(---) : a. s. e. having orthorhomb.symm.+non-zero  $\rho$  and  $\alpha$

(-o-o-) : a. s. e. having orthorhomb. symm + a.a.e. + non-zero  $\rho$  and  $\alpha$  (See Text)

where  $q$  and  $p$  are given by  $q = -1 - \Delta$  and  $p = -1 + \Delta$  in order to maintain a zero trace operator. The angles  $\theta$  and  $\phi$  define the orientation of the magnetic field  $H_0$  with respect to crystallographic axes and  $\gamma'$  is the angle between  $H_0$  and  $Z$  (Figure 3). It has been customary to assume that the principal axes of the a.s.e. and g-tensors are coincident. The purely secular part is given by

$$M_2'(0) = \frac{3S(S+1)}{2h^2} \left[ (D_e/3) \left[ (3+\Delta) \cos^2 \gamma' - (1+\Delta) \right] - D_d (3 \cos^2 \theta - 1) \right]^2 \quad (7)$$

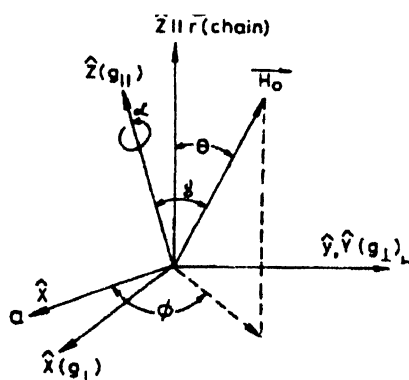


Figure 3. Coordinate system for the theoretical treatment with  $z$  axis along the direction of strong exchange  $\vec{r}(\theta, \phi)$  defining the orientation of applied field  $H_0$  and anisotropic symmetric exchange direction (a.s.e.) is chosen in the  $xz$  plane.

The a.a.e. interaction *i.e.*  $S \times S$  interaction is also described in the coordinates of Figure 3 according to the symmetry rules of Moriya [19]. If  $d$  (antisymmetric exchange vector) lies completely within the  $a$ - $c$  plane, the contribution to the second moment is given by

$$M_2^A = (d^2/8) \{ 2 + \sin^2(\theta - \theta_A) \}, \quad (8)$$

where  $d$  is the scalar magnitude of the antisymmetric exchange interaction and  $\theta_A$  is the angle made by the antisymmetric exchange vector with the  $a$ -axis of the crystal.

Neglecting next-nearest neighbours and hyperfine interactions, the relationship between calculated and observed linewidths is expressed as

$$(\sqrt{3}/2)\Delta H_{pp} = (\sqrt{2}/3J) [M_2' + \rho M_2'(0) + M_2^A]. \quad (9)$$

The adjustable parameters in eq. (9) are  $J$ ,  $D_e$ ,  $\Delta$ ,  $d$ ,  $\theta_A$  and  $\rho$ . The semipositive parameter  $\rho$  enhances the secular interaction *i.e.* when  $\rho = 0$ , secular contributions to  $M_2$  are equally weighted, while for  $\rho > 0$  the secular contributions are preferentially weighted. The experimental linewidth data have been fitted to eq. (9). Since the number of parameters are quite large, we first assume the values of isotropic exchange parameters determined from magnetic susceptibility values and assume only the presence of anisotropic symmetric exchange parameter ( $D_e$ ) having axial symmetry, non-zero  $\rho$  and  $\alpha$  as the three adjustable parameters. The fitting is not at all satisfactory, *i.e.* the fitted curve has curvature opposite to that of experimental curve (Figure 2a). Next assuming a.s.e. to have orthorhombic symmetry *i.e.* non-zero  $\Delta$ , a considerable improvement in the fitting is obtained in that the curvature of the fitted and experimental curves are similar but the fitted  $\Delta H_{pp}$  values are much less than the experimentally obtained values at most of the orientations. With a view to obtain further improvement in fitting, a.a.e. parameter ( $d$ ) is also considered. Remarkable improvement in fitting is obtained in that the fitted and experimental curves are almost coincident. The fitted parameters  $D_e$ ,  $\alpha$ ,  $\rho$ ,  $\Delta$  and  $d$  have also provided quite satisfactory fitting in two other planes, namely (100) and (001) of the crystals (Figure 2b). To verify the authenticity of our fitting, linewidths obtained in another plane (101) are also fitted employing eq. (9) and the above fitted parameters and the fitting is quite excellent (Figure 2c). It is observed that the fitting is most satisfactory when the  $z$ -directions of the a.s.e. and of the a.a.e. tensors are chosen along the chain axis ( $c$ -axis), and the  $b$ -axis ( $\theta_A = 90^\circ$ ) respectively. The best fitted parameters are shown in Table 2. The non-zero values of  $\rho$  *i.e.* 0.20 shows some enhancement of the secular contribution to the second moment. It is also noted that a.s.e. tensor has appreciable orthorhombicity in CHAB ( $\Delta = 1.00$ ). Values of  $D_e$  and  $d$  can be estimated with the help of well-known Moriya relation [19]:

$D_e = (\Delta g/g)^2 J$  and  $d = (\Delta g/g) J$  where  $\Delta g$  is the difference of mean  $g$ -value from the free electron  $g$  value ( $g_e$ ). The values are shown within parentheses in Table 2. It is obvious that Moriya relations fail to account for the fitted values of  $D_e$  and  $d$  obtained from linewidth analysis. It is significant to note here that the present system studied is a halogen co-ordinated Cu(II) compound and halogen  $\text{Br}^-$  has a large spin-orbit coupling compared to that of  $\text{Cu}^{2+}$  ion (for  $\text{Br}^-$  it is  $2200 \text{ cm}^{-1}$  more than that for  $\text{Cu}^{2+}$  which is  $-830 \text{ cm}^{-1}$ ). Since the exchange interactions take place through the intermediary halogen ligand atoms, it is

Table 2. Best fitted parameters for cyclohexylammonium copper bromide (CHAB).

Compound	$J$ ( $\text{cm}^{-1}$ )	$D_e$ ( $\text{cm}^{-1}$ )	$\Delta$ ( $\text{cm}^{-1}$ )	$\alpha$ ( $^\circ$ )	$d$ ( $\text{cm}^{-1}$ )	$\theta_A$ ( $^\circ$ )	$\rho$
CHAB	38.5	1.21	1.00	83.00	1.47	90	0.20
	(37.8;38.5)*	(0.13)**			(2.21)**		

\* Values in parentheses are obtained from magnetic susceptibility and specific heat studies [11, 12, 14]

\*\* Values in parenthesis are obtained by Moriya relation [20]

possible that ligand spin-orbit coupling has some important role to play in determining superexchange and hence the strengths of the different kinds of exchange parameters. For bromine coordinated Cu(II) compounds, in addition, charge transfer interaction may also be involved in the super-exchange process. From above, it is evident that the Moriya relations require modification for a proper description of anisotropic exchange interactions present in halogen coordinated CHAB and similar systems.

#### References

- [1] D Gatteschi and R Sessoli *Mag. Res. Rev.* **15** 1 (1990)
- [2] R D Willet, D Gatteschi and O Kahn (Ed) *Magneto Structural Correlations in Exchange Coupled Systems* (Dordrecht: D Reidel) p241 p269 (1985)
- [3] B R Patyal and R D Willet *Mag. Res. Rev.* **15** 47 (1990)
- [4] H Benner *Phys. Rev.* **B18** 319 (1978)
- [5] A Lagendijk *Phys. Rev.* **B18** 1322 (1978)
- [6] A Lagendijk *Physica (Utrecht)* **83B/C** 283 (1976)
- [7] P M Richards *Phys. Rev.* **B13** 458 (1976)
- [8] K T McGregor and Z G Soos *J. Chem. Phys.* **64** 2506 (1976)
- [9] G C De Vries, R B Helmholtz, E Frikkee, K Kopinga, W J M de Jonge and E F Godefroi *J. Phys. Chem. Solids* **48** 803 (1987)
- [10] H A Groenendijk, H W J Blote, A J Vanduyneveldt, R M Gaura, C P Landee and R D Willett *Physica* **106B** 47 (1981)
- [11] R Hoogerbeets, E H Abu Bakr and A J van Duyneveldt *Physica* **128B** 161 (1985)
- [12] K Kopinga, A M C Tinus and W J M de Jonge *Phys. Rev.* **B25** 4685 (1982)
- [13] A C Phaff, C H W Swuste, W J M de Jonge, R Hoggerbeets and A J van Duyneveldt *J. Phys.* **C17** 2583 (1984)
- [14] M B Ritter, J E Drumheller, T M Kite, I O Snively and K Emerson *Phys. Rev.* **B28** 4949 (1983)
- [15] J A Atamburu and M Moreno *J. Chem. Phys.* **83** 6073 (1985)
- [16] P W Anderson and P R Weiss *Rev. Mod. Phys.* **25** 269 (1953)
- [17] R Kubo and K Tomita *J. Phys. Soc. Jpn.* **9** 888 (1954)
- [18] M Blume and J Hubbard *Phys. Rev.* **B1** 3815 (1970)
- [19] T Moriya *Phys. Rev.* **120** 91 (1960)